J. Fluid Mech. (2005), *vol.* 535, *pp.* 245–254.
doi:10.1017/S0022112005004994 Printed in the United Kingdom

The growth of a mixing layer in a laminar channel

By JAVIER JIMÉNEZ

School of Aeronautics, Universidad Politécnica de Madrid, 28040 Madrid, Spain
and Centre for Turbulence Research, Stanford University

(Received 9 March 2005 and in revised form 19 April 2005)

The effect of the wall-normal diffusion on the spanwise spreading of a steady passive scalar interface is computed for a laminar channel in which the Péclét number, Pe, is high but the velocity profile is parabolic. Two regimes are found according to whether the dimensionless streamwise coordinate $\widetilde{x}$ is smaller or larger than Pe. In both cases the mixing layer spreads as $\widetilde{x}^{1/2}$ to the lowest approximation in Pe^{-1}, although with different numerical coefficients. When $\widetilde{x} \ll Pe$ there is a faster growth of order $\widetilde{x}^{1/3}$ that is restricted to boundary layers near the wall. The intermediate region between those two limits is universal, and is computed numerically. Quantitative results are given that should be useful to experimentally measure diffusion coefficients. The results are easily generalizable to other velocity profiles.

1. Introduction

Taylor (1953, 1954) showed in two classic papers that the effective diffusion coefficient of a solute is enhanced when the mixing occurs in a sheared flow. His analysis deals with the experimentally important case in which the solute is injected as a plug filling a tube, and the diffusion is nominally streamwise. It therefore competes with the advection by the sheared streamwise velocity, which generates a wall-normal concentration gradient that is responsible for the increased diffusion. A different experimental configuration has recently become common in which the diffusion happens in a narrow channel where two streams of different solute concentrations are injected side by side in the spanwise direction. That configuration has for example been used to measure diffusion coefficients and reaction parameters between different species (Ismagilov *et al.* 2000; Kamholz & Yager 2001; Baroud *et al.* 2002). The conditions are such that, although the Reynolds number is low enough for the flow to remain laminar, so that the mean velocity profile stays approximately parabolic, the Péclét number, Pe, of the solute is large, and the lateral diffusion occurs slowly. Since the evolution of the mixing layer is then also slow, its growth is also modified by the interaction with the streamwise shear. It is for example clear that, were it not for the wall-normal diffusion, the mixing layer would grow at different rates at different wall distances, corresponding to the different local velocities.

This configuration has been analysed qualitatively in the chemical literature, with results which generally agree with those obtained below. Kamholz *et al.* (1999) argued for example that the diffusion laws are different when the streamwise development length is small or large, and that the criterion separating the two regions is the Péclét number. They analysed the far-downstream case, and concluded that the layer grows there as if the flow were uniform with the bulk velocity. Ismagilov *et al.* (2000)

concentrated on the upstream region and noted that the spreading law near the wall had then to be different from that in the core of the channel. They generalized Levèque's (1928) analysis of diffusion in a shear (see Schlichting 1979) to show that the layer should spread near the wall as the cube root of the downstream coordinate, but that at the centre of the channel it should follow the more classical square-root law. They documented the two spreading exponents in their experimental channel. Kamholz & Yager (2002) have more recently presented a numerical calculation of the flow that is essentially equivalent to the one given below in § 2, and which confirms the previous qualitative conclusions. They however apparently failed to realize that the problem is parameter-free, and that their solution could be applied to any channel with a parabolic profile as long as the dimensionless distance is of the order of Pe.

The purpose of the present paper is to analyse quantitatively the steady mixing layer in the idealized case in which the velocity profile is parabolic, and the solute is diluted enough for the diffusion to be Fickian. We will show that the problem can be expressed to lowest approximation in a universal form, and we will give solutions in enough detail to allow the experimental arrangement to be used in the determination of molecular diffusion coefficients. Special emphasis will be put on the two asymptotic limits in which the downstream dimensionless distance is much smaller or much greater than the Péclét number, which are difficult to treat as part of the numerical simulation mentioned above.

A secondary motivation for this paper is the recent identification of two coexisting spreading laws in the spectral density of the streamwise velocity fluctuations in turbulent wall flows. It was shown by del Álamo *et al.* (2004) and by Jiménez, del Álamo & Flores (2004) that those spectra contain relatively narrow ridges at long wavelengths, scaling as $\lambda_z \sim \lambda_x^{1/3}$ in the viscous and buffer sublayers, and as $\lambda_z \sim \lambda_x^{1/2}$ in the logarithmic region. By interpreting the wavelengths λ_x and λ_z as characteristic streamwise and spanwise dimensions of individual velocity structures, those authors suggested that the above laws could be explained by the spreading of wakes left in the mean velocity profile by compact wall-normal-velocity structures.

It has often been noted that, for long streamwise structures, the equations for the streamwise and for the transverse velocity components approximately decouple, and that the former can be approximated as a passive species advected by the latter (Orlandi & Jiménez 1994). In a turbulent flow this advection can be represented as a turbulent diffusion, and it was shown by del Álamo *et al.* (2004) that reasonable assumptions on the advection velocity of the generating structures and on the effective eddy viscosity yield spreading rates which agree quantitatively with the spectral square-root behaviour observed in the logarithmic layer. It was also noted by Jiménez *et al.* (2004) that the conditions of uniform shear and constant diffusion coefficient required for the cube-root diffusion law cited above are reasonable assumptions near the wall. Finally, the physical structure of the wakes in the logarithmic region was isolated by means of conditional statistics in del Álamo *et al.* (2005), and supporting evidence for wakes in the buffer layer was provided by Jiménez *et al.* (2004).

Diffusion in turbulent flows is complicated by the spatial variability of the eddy viscosity, and the comparison between theory and experiments is weakened by the doubtful nature of the eddy-viscosity model itself. That question will therefore not be pursued further, and the extent to which we will consider this secondary problem here will only be to document the interaction of the two spreading laws in a simple setting in which the underlying equations are well defined, and where the experimental comparison can be carried out unambiguously.

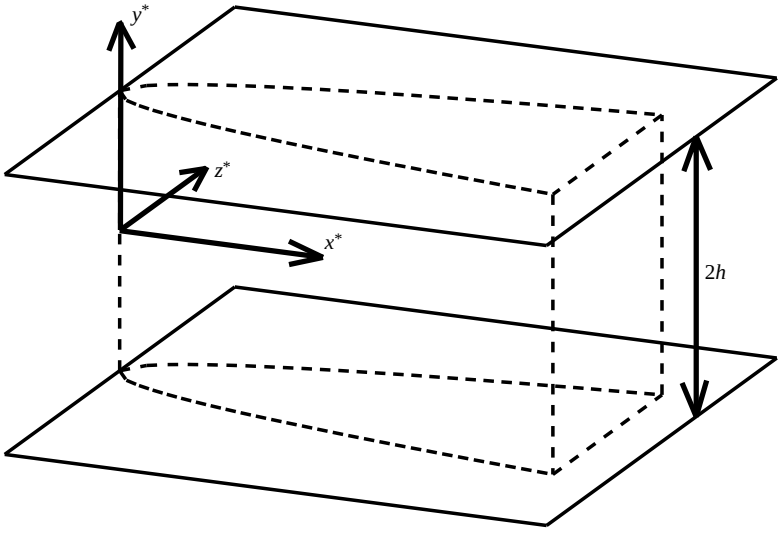

FIGURE 1. Problem geometry.

The structure of the paper is as follows. The basic equations are defined in § 2, which also contains the numerical integration of the reduced universal problem. The near- and far-field limits of that solution are analysed in §§ 3 and 4, and the conclusions are summarized in § 5. A preliminary version of this work appeared in Jiménez (2004), but the reader is warned that it contained incorrect notation and minor factual errors that were pointed out during the refereeing of this paper, and which have now been corrected.

2. Basic scaling

Consider a channel between two infinite parallel plates located at $y^* = \pm h$, and assume that its velocity profile is parabolic (see figure 1). Normalize the velocity U^* with its maximum U_c, and the coordinates with h, so that $U = 1 - \widetilde{y}^2$, where $\widetilde{y} = y^*/h$ and $U = U^*/U_c$. Denote by $\widetilde{x}$ and $\widetilde{z}$ the streamwise and spanwise coordinates, normalized in a similar way. Two streams with different concentrations of a passive scalar c are initially at $\widetilde{z} > 0$ and $\widetilde{z} < 0$, and come together at $\widetilde{x} = 0$. The diffusion equation for c is

$$Pe\,(1-\widetilde{y}^2)\partial_{\widetilde{x}} c = \partial_{\widetilde{x}\widetilde{x}} c + \partial_{\widetilde{y}\widetilde{y}} c + \partial_{\widetilde{z}\widetilde{z}} c, \tag{2.1}$$

where $Pe = U_c h/\kappa \gg 1$, and κ is the diffusivity of c. We will assume that there is no diffusion flux into the walls, so that

$$\partial_{\widetilde{y}} c = 0 \text{ at } \widetilde{y} = \pm 1, \tag{2.2}$$

and that the mixing takes place between

$$c \to \pm 1/2 \text{ as } \widetilde{z} \to \pm\infty. \tag{2.3}$$

As long as $\widetilde{x} \gg 1$ the streamwise diffusion term is negligible with respect to the other two directions, and can be neglected. The spreading of the mixing layer involves the balance of the streamwise advection with the spanwise diffusion, which have to be of the same order. If $\widetilde{x} = O(L)$, the spanwise scale then has to be $\widetilde{z} = O(L/Pe)^{1/2}$, and

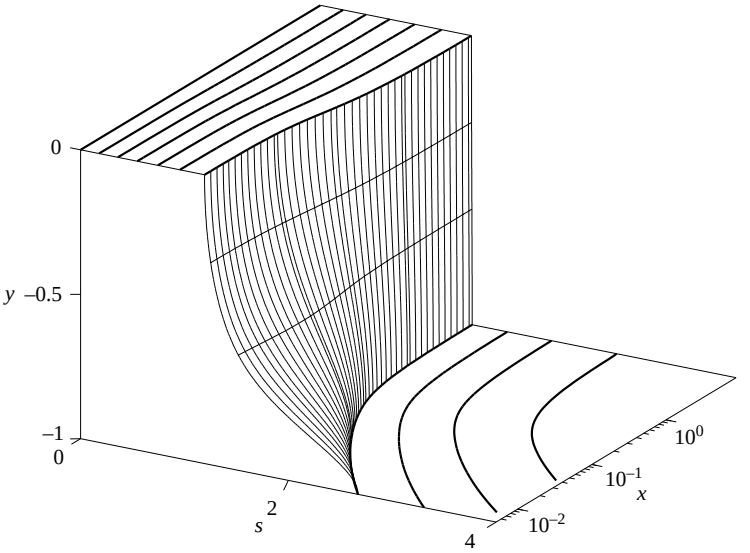

FIGURE 2. Numerical solution of (2.6), for $s > 0$ and $y < 0$. The wall is at the bottom, and the channel centre at the top. The flow is from bottom left to top right. The isosurface represented is $c = 0.3$. The isolines on the top plane are $c = 0.05(0.05)0.3$, and those at the bottom plane are $c = 0.3(0.05)0.45$.

(2.1) becomes

$$(1 - y^2)\partial_x c = (LPe)^{-1}\partial_{xx} c + LPe^{-1}\partial_{yy} c + \partial_{zz} c, \tag{2.4}$$

where $x = \widetilde{x}/L$, $y = \widetilde{y}$, and $z = \widetilde{z}(Pe/L)^{1/2}$.

There is a natural scaling, $L = Pe$, in which the three largest terms of (2.4) are of comparable magnitude. Defining final stretched coordinates

$$x = \widetilde{x}/Pe, \;\; y = \widetilde{y}, \;\; z = \widetilde{z}, \tag{2.5}$$

we obtain

$$(1 - y^2)\partial_x c = \partial_{yy} c + \partial_{zz} c + O(Pe^{-2}). \tag{2.6}$$

The leading order of this equation is parameter-free, and can be integrated numerically. The solution is symmetric with respect to $y = 0$, and antisymmetric with respect to $z = 0$, and is shown in figure 2 as a function of the scaled x, of y, and of the usual similarity variable for two-dimensional diffusion problems

$$s = z/x^{1/2}. \tag{2.7}$$

It has been computed using a second-order Crank–Nicholson marching code, using 200 grid points in y, and between 200 and 800 points in z, depending on the distance to the origin. The step in x was refined to ensure grid independence in the critical region of small x. The solution in the figure corresponds to the overlap of three different computations in three different x-ranges, and the lack of discontinuities between the ranges was used as a criterion for numerical convergence.

It is seen in the figure that the solution follows the square-root law fairly well at the central plane, but that near the wall it spreads faster, specially at the early stages of the mixing. Even at the central plane there is a transition in the growth rate around $x = 1$. As mentioned in the introduction, Kamholz & Yager (2002) discuss a numerical solution of (2.6) which is essentially equivalent to the one in figure 2, although they

present it as applying only to a particular Péclét number. They analyse it in terms of the local growth exponent, which is the logarithmic slope of the growth of the mixing width. They for example describe the transition between the two different growth coefficients near the central plane of the channel as a local growth exponent of 2/3.

The numerical integration cannot be extended in practice to values of x which are much smaller or much bigger than 1, where the layer is either very thin or very thick. To understand those two limits it is easier to consider directly the asymptotic behaviour of the solutions in the two cases.

3. The near limit, $\widetilde{x} \ll Pe$

This is the relevant experimental case when $Pe \gg 1$, unless very long channels are available. When $x \ll 1$, which corresponds to $L \ll Pe$ in (2.4), the longitudinal transport and the transverse diffusion are the dominant terms in (2.6). It is then natural to attempt a representation of this *near* solution c_{near} as an asymptotic series in $L/Pe \ll 1$, each of whose terms would satisfy a diffusion equation in the (x, z)-plane, with small corrections due to the wall-normal diffusion. However, since L/Pe was defined as a measure of the magnitude of x, this suggests an expansion

$$c \equiv c_{near} = c_{n,0} + x c_{n,1} + \ldots + x^N c_{n,N} + O(x^{N+1}), \tag{3.1}$$

for some chosen asymptotic order N. The coefficients $c_{n,k}$ are functions of y and of s. They satisfy

$$\partial_{ss} c_{n,k} + (1 - y^2)\left(\frac{s}{2}\partial_s c_{n,k} - k c_{n,k}\right) = -\partial_{yy} c_{n,k-1}, \tag{3.2}$$

where $c_{n,0}$ satisfies the boundary conditions (2.3), and all the higher-order terms vanish as $z \to \pm\infty$. This is a well-ordered hierarchy of equations for $c_{n,k}$ in which y appears only as a parameter or in a right-hand side that depends on the solution $c_{n,k-1}$ of a previously obtained member of the hierarchy. In the leading-order equation

$$\partial_{ss} c_{n,0} + (1 - y^2)\frac{s}{2}\partial_s c_{0,k} = 0, \tag{3.3}$$

the right-hand side vanishes, and the solution can be written immediately as

$$c_{n,0} = \tfrac{1}{2}\mathrm{erf}(Z/2), \tag{3.4}$$

where

$$Z = s(1 - y^2)^{1/2}. \tag{3.5}$$

Equation (3.4) satisfies the boundary conditions for c at $z \to \pm\infty$, but not the zero-flux conditions (2.2) at the walls.

Consider the neighbourhood of the lower wall, and define the distance to the wall as $y' = y + 1$. When $y' \ll 1$ the velocity is $U \approx 2y'$, and $c_{n,0}$ behaves as $y'^{1/2}$. In this region the width of the mixing layer given by (3.4) is $z = O([x/y']^{1/2})$, and there is a boundary layer of thickness $y' = O(x^{1/3})$ in which the wall-normal diffusion cannot be neglected. There are then new similarity variables

$$\eta = y'/x^{1/3}, \tag{3.6}$$

and

$$\zeta = z/x^{1/3}, \tag{3.7}$$

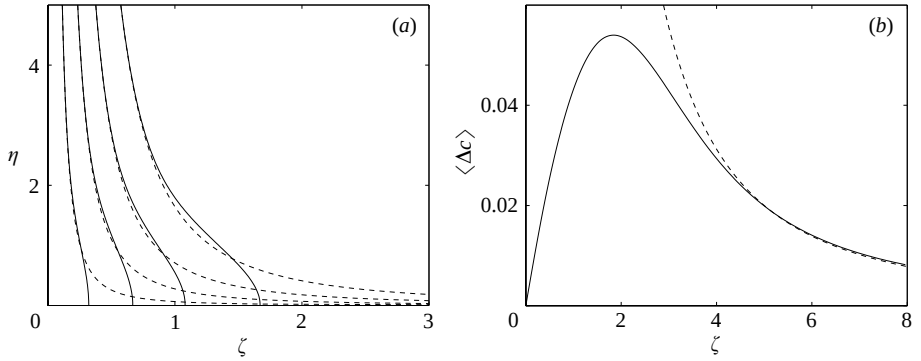

FIGURE 3. (*a*) Similarity solution for the boundary layer near the lower wall. ——, Similarity solution; – – –, outer solution (3.9). The contours are $c_{BL}=0.1(0.1)0.4$. (*b*) Correction to the vertically integrated concentration due to the boundary layer. ——, $\langle c_{BL}-c_{n,0}\rangle$; – – –, large-$\zeta$ limit, $0.5/\zeta^2$.

in terms of which (2.6) becomes

$$\partial_{\eta\eta}c+\partial_{\zeta\zeta}c+\tfrac{2}{3}\eta(\eta\partial_\eta c+\zeta\partial_\zeta c)=O\left(x^{1/3}\right). \tag{3.8}$$

The error term on the right-hand side is due primarily to the expansion of U near the wall in terms of η. The concentration c must satisfy (2.2) at $\eta=0$, and (2.3) at $\zeta=\pm\infty$. It also has to match, when $\eta\gg1$, the $y'\ll1$ limit of the outer solution (3.4),

$$c_{n,0}\approx\tfrac{1}{2}\mathrm{erf}\left[\zeta(\eta/2)^{1/2}\right]. \tag{3.9}$$

This is a parameter-free elliptic problem that can be solved numerically. Its solution, c_{BL}, is antisymmetric with respect to $\zeta=0$, and is shown graphically in figure 3(*a*). It has been obtained in the domain $\zeta=(0,\ 8)$ and $\eta=(0,\ 6)$, using a straightforward second-order finite-difference code with a grid of 200×250 points. It tends to (3.9) away from the wall, but it has a finite width in ζ at the wall.

Note that the higher-order terms of the outer expansion for c_{near} become increasing singular near the wall. While the only singularity of $c_{n,0}$ comes from the similarity variable Z, the next term,

$$c_{n,1}=-\frac{Z(3+3y^2+y^2Z^2)}{12\sqrt{\pi}(1-y^2)^3}\exp(-Z^2/4), \tag{3.10}$$

has an extra factor factor y'^{-3}. It is easy to show that $c_{n,k}x^k$ behaves near the wall as $(x/y'^3)^k=\eta^{-3k}$. Since Z is also approximately $\zeta\eta^{1/2}$ in that limit, it follows that the inner limit of the outer solution is a function of ζ and η which has contributions from all the orders in the expansion (3.1). It is however clear from the previous discussion that the contributions to this function of the higher-order terms decay quickly as η increases, and that the boundary-layer solution can be matched safely to $c_{n,0}$ as long as the matching is done far enough away. On the other hand, this is a problem in which the only way to avoid singularities in the higher-order terms is to use in the right-hand side of (3.2) the composite solutions formed by the lower-order boundary-layer and outer solutions, instead of just by the outer ones (Van Dyke 1964). This has no effect in the outer region, where the inner and outer solutions coincide but, within the boundary layer where $\partial_{yy}c_{BL}=O(x^{-2/3})$, the correction xc_1 is $O(x^{1/3})$. This was already suggested by the right-hand side of (3.8).

What is often measured in experiments is the vertically integrated concentration

$$\langle c \rangle = \frac{1}{2} \int_{-1}^{1} c \, \mathrm{d}y. \tag{3.11}$$

Using (3.4), it can be written in the present case as

$$\langle c \rangle \approx \langle c_{n,0} \rangle + x^{1/3} \langle \Delta c \rangle = \frac{\sqrt{\pi}}{8} s \exp(-s^2/8)[\mathrm{I}_0(s^2/8) + \mathrm{I}_1(s^2/8)] + x^{1/3} \langle \Delta c \rangle, \tag{3.12}$$

where I_0 and I_1 are Bessel functions. The correction $\langle \Delta c \rangle$ due to the boundary layers is

$$\langle \Delta c \rangle(\zeta) = \int_0^{\infty} (c_{BL} - c_{n,0}) \, \mathrm{d}\eta, \tag{3.13}$$

and is given in figure 3(*b*). For $\zeta \gg 1$ the solution c_{BL} is everywhere close to its asymptotic value 1/2, and (3.13) is mostly due to the integral of $1/2 - c_{n,0}$, which can be evaluated exactly. That limit, $\langle \Delta c \rangle \approx 1/2\zeta^2$, is included in figure 3(*b*) for comparison.

Because $\langle c_{n,0} \rangle(s)$ and $\langle \Delta c \rangle(\zeta)$ depend differently on x it is impossible to express the composite solution in terms of a single similarity variable but, since (3.12) and (3.13) only hold in the limit $x \ll 1$, it is usually possible to write asymptotically valid expressions for most quantities. Consider for example the dimensionless 'slope' thickness defined by

$$\delta_s = \delta_s^*/h = \frac{c_\infty - c_{-\infty}}{\langle c \rangle_z'} \tag{3.14}$$

where c_z' stands for $\partial_z c$ at $z = 0$. Using the expressions above,

$$\delta_{s,near}^{-1} = \langle c_{n,0} \rangle_s' x^{-1/2} + \langle \Delta c \rangle_\zeta' \approx \frac{\sqrt{\pi}}{8} x^{-1/2} + 0.0551, \tag{3.15}$$

where $\langle c_{n,0} \rangle_s'$ follows from (3.12), and $\langle \Delta c \rangle_\zeta'$ has been estimated numerically from figure 3(*b*). Similar expressions can be obtained for other product thicknesses.

4. The limit $\tilde{x} \gg Pe$

When $x \gg 1$, the mixing layer becomes much wider than h, and the dominant diffusion term is the one normal to the wall. In this *far* region, the natural expansion is an asymptotic series in powers of the small quantity Pe/L which, as in the previous section, is actually an expansion in inverse powers of x,

$$c \equiv c_{far} = c_{f,0} + x^{-1} c_{f,1} + \ldots + x^{-N} c_{f,N} + O(x^{-N-1}), \tag{4.1}$$

where the coefficients are again functions of s and y, and satisfy

$$\partial_{yy} c_{f,k+1} = -\partial_{ss} c_{f,k} - (1 - y^2) \left(\frac{s}{2} \partial_s c_{f,k} + k c_{f,k} \right). \tag{4.2}$$

To leading order, $\partial_{yy} c_{f,0} = 0$ and, from the boundary conditions (2.2), it follows that $c_{f,0}$ is only a function of s. To obtain it we must enforce a compatibility condition from the next order, where

$$\partial_{yy} c_{f,1} = -(1 - y^2) \frac{s}{2} \partial_s c_{f,0} - \partial_{ss} c_{f,0}. \tag{4.3}$$

The correction $c_{f,1}$ has to satisfy the Neumann conditions (2.2) at $y = \pm 1$, and it follows from the integration of (4.3) between the two walls that this is only possible

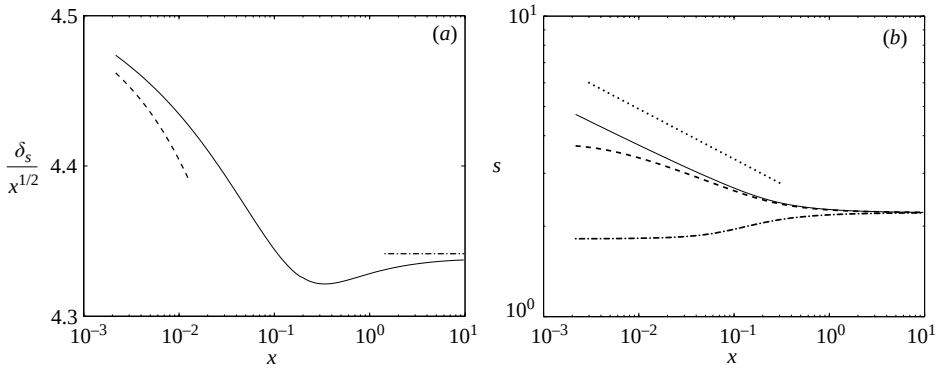

FIGURE 4. (*a*) Slope thickness of the mixing layer, scaled with $x^{1/2}$. ———, Numerical result; — — —, small-x limit (3.15); — · —, large-x limit (4.6). (*b*) Lateral position of the isosurface $c = 0.4$, scaled with $x^{1/2}$, for different wall distances. ———, $y' = 0.01$; — — —, $y' = 0.15$; — · —, central plane. $y' = 1$. The dotted line corresponds to $z \sim x^{1/3}$.

if

$$\langle (1-y^2) \rangle \frac{s}{2} \partial_s c_{f,0} + \partial_{ss} c_{f,0} = \frac{s}{3} \partial_s c_{f,0} + \partial_{ss} c_{f,0} = 0, \tag{4.4}$$

from where we write immediately

$$c_{f,0} = \langle c_{f,0} \rangle = \tfrac{1}{2} \mathrm{erf}(s/\sqrt{6}). \tag{4.5}$$

Note that the similarity variable in (4.5) is the same as the one for $\langle c_{n,0} \rangle$ in the previous section, but that the spreading rate is different. The first-order correction $c_{f,1}$ can be obtained by integrating (4.3) with respect to y, and contains an unknown additive function of s that has to satisfy a diffusion equation similar to (4.4), but the solution is now uniformly valid across the channel, and the correction is everywhere $O(x^{-1})$. To leading order, the slope thickness of the mixing layer is

$$\delta_{s,far} = (6\pi x)^{1/2}. \tag{4.6}$$

In figure 4(*a*) the evolution of the slope thickness obtained from the numerical solution of (2.6) is compared to the asymptotic expressions (3.15) and (4.6). The approximation is much better in the downstream limit than in the one near the origin, in agreement with the different orders of the corrections which have been neglected, but the solution deviates little in general from a square-root growth law.

Note that we could have written the similarity variable s in the far region with an arbitrary shift in the origin of x, since the approximation in this section does not hold at the physical origin of the mixing region. Any shift in the virtual origin can however be expected to be at most $O(1)$, and would only appear in a large-x expansion as a term of $O(x^{-1})$.

The growth of the mixing layer at different distances from the wall is summarized in figure 4(*b*), which is compiled from the numerical results. The square-root growth appears as constant in this plot, and it is followed by the layer at the central plane. The two different constants at small and large downstream locations correspond to the two outer solutions (3.9) and (4.5). Near the wall the layer follows initially the $x^{1/3}$ growth law, and only joins the square-root behaviour when the mixing layer becomes vertically uniform farther downstream. The behaviour of the intermediate location at $y' = 0.15$ is interesting. It is initially in the outer core of the channel, where it follows approximately the square-root law. It then changes to an $x^{1/3}$ behaviour as

it is swallowed by the growth of the wall boundary layer, and it only returns to $x^{1/2}$ in the downstream limit in which the layer becomes uniform.

5. Conclusions

We have shown that the spreading of a spanwise discontinuity of a passive scalar in a laminar channel is modified by the wall-normal diffusion due to the variation of the advection velocity with the distance to the wall. The spreading in the central plane is always approximately like $(\tilde{x}/Pe)^{1/2}$, but the constant is different near the origin and far downstream. Near the origin the wall-normal diffusion is negligible in this central region, but it becomes dominant far downstream, where the layer is much wider than the channel thickness. The layer then becomes uniform in the wall-normal direction, and behaves as if the advection velocity were constant and equal to the bulk velocity.

Near the origin the wall-normal diffusion is only important in boundary layers that develop near each wall. They have widths and heights of the order of $(\tilde{x}/Pe)^{1/3}$, and they account for corrections of that order to the square-root behaviour of the vertically integrated scalar profiles. The transition between the two regimes occurs at $\tilde{x} \approx Pe$, when the wall layers fill the whole channel. We have given numerical results which can be used to interpret experiments.

Because the shear is orthogonal to the spreading, its effect on the vertically averaged concentration profile is weaker than in the better-known case of the longitudinal diffusion of a plug in a tube. While in that case the effective diffusion coefficient increases without bound with the Péclét number (Taylor 1953), here the maximum difference is between the asymptotic laws (3.15) and (4.6), which correspond to an effective advection velocity $\pi^2 U_c/16 \approx 0.62 U_c$ near the origin, and to the bulk velocity $2U_c/3$ far downstream. The resulting change of the averaged spreading rate is less than 5%. Other experimental configurations would be more sensitive to this effect. We have already mentioned that differentiating the present analysis with respect to z gives the spreading of a scalar injected from a line source aligned with the y-axis. Injecting the scalar from a point at one wall, on the other hand, would result in an $x^{1/3}$ initial spreading as long as the plume stays close to the wall, changing later to $x^{1/2}$ as it penetrates into the core region. The turbulent wakes mentioned in the introduction are presumably closer to this configuration.

Real experimental channels do not have infinite span, and their profiles are not always completely developed. Their velocity is then not exactly parabolic, but most of the previous analysis applies to them with few changes. In the far region, equation (4.4) applies to any velocity profile, with the only difference being how the bulk velocity is determined. In the region $x \ll 1$, the second factor in the core similarity variable (3.5) is the square root of the velocity, and this also holds for any profile. In the boundary layers of that region, the velocity profile only enters as the approximation $U \approx 2y'$, and the analysis can be extended to other cases by substituting the numerical coefficient 2/3 in front of the last term in the left-hand side of (3.8) by $U'(0)/3$.

Other extensions are not so trivial. The information obtained here on the diffusion of a solute is enough to compute the product thickness of a fast chemical reaction, such as those often used as tracers (Liñán & Williams 1993), but the generalization to several solutes or reaction products with different diffusion coefficients is not easy, and introduces extra parameters. It will not be pursued here.

This work was supported in part by CICYT, under grant BPI2003-03434, and by the US Department of Energy under the ASC program.

REFERENCES

del Álamo, J. C., Jiménez, J., Zandonade, P. & Moser, R. D. 2004 Scaling of the energy spectra of turbulent channels. *J. Fluid Mech.* **500**, 135–144.

del Álamo, J. C., Jiménez, J., Zandonade, P. & Moser, R. D. 2005 Attached and detached vortex clusters in the logarithmic region. *J. Fluid Mech.* (submitted).

Baroud, C. N., Okkels, F., Ménétrier & Tabeling, P. 2002 Reaction-diffusion dynamics: Confrontation between theory and experiment in a microfluidic reactor. *Phys. Rev.* E **67**, 060104-1.

Ismagilov, R. F., Strook, A. D., Kenis, P. J. A., Whitesides, G. & Stone. H. A. 2000 Experimental and theoretical scaling laws for transverse diffusive broadening in two-phase laminar flows in microchannels. *Appl. Phys. Lett.* **76**, 2376–2378.

Jiménez, J. 2004 Spreading laws for diffusion in a low-Reynolds-number channel. *CTR Res. Briefs, Stanford University*, pp. 223–230.

Jiménez, J., del Álamo, J. C. & Flores, O. 2004 The large-scale dynamics of near-wall turbulence. *J. Fluid Mech.* **505**, 179–199.

Kamholz, A. E., Weigl, B. H., Finlayson, B. A. & Yager, P. 1999 Quantitative analysis of molecular interaction in microfluidics channels: the T-sensor. *Anal. Chem.* **71**, 5340–5347.

Kamholz, A. E. & Yager, P. 2001 Theoretical analysis of molecular pressure-driven laminar flow in microfluidics channels. *Biophys. J.* **80**, 155–160.

Kamholz, A. E. & Yager, P. 2002 Molecular diffusive scaling laws in pressure-driven microfluidics channels: deviation from one-dimensional Einstein approximations. *Sensors and Actuators* B **82**, 117–121.

Levèque, M. A. 1928 Les lois de la transmission de chaleur par convection. *Ann. Mines* **13**, 201–239.

Liñán, A. & Williams, F. A. 1993 *Fundamental Aspects of Combustion*, pp. 63–65. Oxford University Press.

Orlandi, P. & Jiménez, J. 1994 On the generation of turbulent wall friction. *Phys. Fluids* **6**, 634–641.

Schlichting, H. 1979 *Boundary Layer Theory*, pp. 291–292. McGraw-Hill.

Taylor, G. I. 1953 Dispersion of soluble matter in solvent flowing slowly through a tube. *Proc. R. Soc. Lond.* A **219**, 186–203.

Taylor, G. I. 1954 Conditions under which a solute in a stream of solvent can be used to measure molecular diffusion. *Proc. R. Soc. Lond.* A **225**, 473–477.

Van Dyke, M. 1964 *Perturbation Methods in Fluid Mechanics*, pp. 93–97. Academic.